Bergische Universität Wuppertal

Fakultät für Mathematik und Naturwissenschaften

Institute of Mathematical Modelling, Analysis and Computational Mathematics (IMACM)

Preprint BUW-IMACM 23/08

Manh Tuan Hoang and Matthias Ehrhardt

A dynamically consistent nonstandard finite difference scheme for a generalized SEIR epidemic model

June 23, 2023

http://www.imacm.uni-wuppertal.de

A dynamically consistent nonstandard finite difference scheme for a generalized SEIR epidemic model

Manh Tuan Hoang[a,*], Matthias Ehrhardt[b,**]

[a] *Department of Mathematics, FPT University, Hoa Lac Hi-Tech Park, Km29 Thang Long Blvd, Hanoi, Viet Nam*
[b] *University of Wuppertal, Chair of Applied and Computational Mathematics, Gaußstrasse 20, 42119 Wuppertal, Germany*

Abstract

This work is devoted to the proposal and analysis of a new mathematical study of the transmission dynamics of infectious diseases. First, a generalized SEIR epidemic model is presented that uses general nonlinear incidence rates to describe the "psychological" effect. Then, a rigorous mathematical analysis is performed for the proposed SEIR model. We establish positivity and boundedness, calculate the basic reproduction number, determine possible equilibrium points (disease-free and endemic), and investigate their asymptotic stability properties of the SEIR model. The obtained results improve and extend a SEIR model constructed in a recent work; moreover, the proposed model is useful for studying the COVID-19 epidemic in particular and other infectious diseases in general.

For the purpose of numerical simulation, the Mickens method is applied to construct a dynamically consistent non-standard finite difference (NSFD) model for the proposed SEIR epidemic model. The constructed NSFD scheme is able to provide reliable approximations that not only preserve the dynamic properties of the SEIR model for all values of the step size, but also are easy to implement.

Finally, a series of illustrative numerical experiments are performed to support the theoretical findings and confirm the advantages of the NSFD

---

[*] Corresponding author
[**] Corresponding author
Email addresses: `tuanhm14@fe.edu.vn`; `hmtuan01121990@gmail.com` (Manh Tuan Hoang), `ehrhardt@uni-wuppertal.de` (Matthias Ehrhardt)

scheme over some well-known standard methods.

Keywords: Infectious diseases, COVID-19, Dynamical analysis, Basic reproduction number, NSFD schemes
2010 MSC: 37M05, 37M15, 65L05, 65P99

1. Introduction

Mathematical modeling and analysis of infectious diseases has become a fundamental and indispensable approach for discovering the characteristics and mechanisms of epidemics as well as for predicting possible scenarios in reality [7, 8, 42]. The study of mathematical models of infectious diseases can provide us with appropriate strategies for disease control and prevention. This is of great benefit to public health and health care. For this reason, in an effort to model the COVID-19 epidemic, many mathematicians and epidemiologists have proposed and analyzed a large number of mathematical models describing the transmission dynamics of COVID-19 (see, e.g. [2, 17, 31, 33, 47, 53, 48, 51, 58] and references therein). Measures to mitigate and prevent COVID-19 outbreaks have been proposed as an important consequence. Recently, we performed a mathematical study on the transmission dynamics of SARS-CoV-2 with waning immunity [20].

We now adopt an accepted mathematical model of the 2019 coronavirus epidemic (COVID-19) proposed by Rohith and Devika [53]. The model is represented by a system of nonlinear differential equations:

$$\begin{aligned}
\dot{S} &= \mu - \frac{\beta_0 SI}{1+\alpha I^2} - \mu S,\\
\dot{E} &= \frac{\beta_0 SI}{1+\alpha I^2} - (\sigma+\mu)E,\\
\dot{I} &= \sigma E - (\gamma+\mu)I,\\
\dot{R} &= \gamma I - \mu R.
\end{aligned} \tag{1}$$

In this model, the total population is divided into four classes according to the status of individuals with respect to COVID-19, i.e., susceptible (S), exposed (E), infected (I), and removed (R); the birth/death rate is represented by μ; γ is the recovery rate; and σ is the measure of the rate at which exposed individuals become infected. We refer readers to [53] for more details of the model (1). In [53], the bifurcation analysis and control problem for the model

(1) were thoroughly studied. Although the (2) model was proposed to study the transmission dynamics of the COVID-19 epidemic, it is also very useful for studying other infectious diseases.

Setting in the nonlinear incidence rate $\frac{\beta_0 SI}{1+\alpha I^2}$, $\psi(I) = 1+\alpha I^2$, the denominator $\psi(I)$ satisfies the following properties

(H1) $\psi(0) = 1$;

(H2) $\psi(I) > 0$ for $I > 0$;

(H3) $\psi'(I) \geq 0$ for $I \geq 0$.

Remark 1. *The family of nonlinear incidence rates satisfying the conditions (H1)–(H3) was proposed in [34]. These functions are not only biologically motivated and can be used to interpret the "psychological" effect, but also include many well-known incidence functions [23, 34, 37, 38, 39, 59].*

In this paper we consider a generalized version of the model (1) by replacing the function $1 + \alpha I^2$ with general functions satisfying (H1)–(H3). More precisely, we propose the following model

$$\begin{aligned}
\dot{S} &= \mu - \frac{\beta_0 SI}{\psi(I)} - \mu S,\\
\dot{E} &= \frac{\beta_0 SI}{\psi(I)} - (\sigma + \mu)E,\\
\dot{I} &= \sigma E - (\gamma + \mu)I,\\
\dot{R} &= \gamma I - \mu R,
\end{aligned} \tag{2}$$

where $\psi(I)$ is any function satisfying (H1)–(H3). Note that if we set $f(I) = I/\psi(I)$, then

(i) $f(0) = 0$, $f(I) > 0$ for $I > 0$;

(ii) $f(I)/I$ is continuous and monotonously non-increasing for $I > 0$, and $\lim_{I\to 0^+} f(I)/I$ exists, denoted by β, $(0 < \beta < \infty)$;

(iii) $\int_{0^+}^{1} \big(1/f(u)\big)\,du \leq \int_{0^+}^{1} (1/u)\,du = \infty$.

Thus, the function $f(I)$ also satisfies the properties given in [37]. This means that the model (2) is not only a generalization of the model (1), but also includes more epidemic scenarios. This is very useful both in theory and in practice. For this reason, we consider the (1) model in the context of general incidence rates.

In [38, 59], SEIRS in epidemiology with general nonlinear incidence have been considered. However, a key difference between the models (1), (2) and the SEIRS models in [38, 59] is that the derivation of (1) and (2) is explained based on the "psychological" effect and they are proposed to mainly study transmission dynamics of the COVID-19 epidemic.

In the first part of this paper, positivity, boundedness, the basic reproduction number, possible equilibria, and asymptotic stability properties of the model (2) are rigorously analyzed. Using Lyapunov stability theory, it is proved that a unique disease-free equilibrium (DFE) point is globally asymptotically stable if the basic reproduction number $\mathcal{R}_0$ satisfies $\mathcal{R}_0 < 1$; and the disease-endemic equilibrium (DEE) point exists and is locally asymptotically stable if $\mathcal{R}_0 > 1$. Consequently, the qualitative dynamic properties of the model (2) are fully determined and mitigation and prevention measures can be specified. Moreover, the results obtained improve and extend those presented in the comparative work [53] (see Remark 3).

In the second part, we construct a reliable numerical scheme for the purpose of numerical simulation as well as for the construction of scientific computational programs. To achieve this goal, we use the Mickens methodology [43, 44, 45] to formulate a dynamically consistent nonstandard finite difference (NSFD) scheme for the model (2). It is well-known that the main advantage of NSFD schemes over standard schemes is that they can preserve essential mathematical properties of differential equations independent of the values of the step size [43, 44, 45]. Therefore, they are efficient and suitable for simulating the behavior of dynamic differential equation models over long periods of time. Nowadays, NSFD schemes have become an efficient approach for numerically solving real-world problems (see, e.g. [12, 13, 22, 46]). More recently, we have developed the Mickens method to construct NSFD schemes for mathematical models of phenomena and processes in science and technology such as biology, ecology, or other natural sciences [14, 15, 16, 11, 25, 26, 27, 28, 29, 30].

Through rigorous mathematical analysis, we prove that the constructed NSFD scheme can exactly preserve the positivity, boundedness, local asymptotic stability, and especially the global asymptotic stability of the model (2) for all values of the step size. In other words, the NSFD scheme can reproduce the dynamics and therefore behaves similarly to the continuous model.

This is useful for predicting transmission and for representing possible infectious disease scenarios. It is worthy noting that the constructed NSFD scheme can be extended to obtain dynamically consistent NSFD schemes for SEIR models introduced in [38, 59].

In the third part, a series of illustrative numerical experiments are performed to support the theoretical results and demonstrate the advantages of the constructed NSFD scheme over some standard methods. The numerical examples provide convincing evidence confirming the validity of the main results of this work. It is proved that the standard Euler and second-order Runge-Kutta (RK2) schemes can produce numerical approximations that are negative and unstable for certain step sizes. This means that the dynamics of the model (2) cannot be obtained. However, with the NSFD method, the dynamics of (2) is correctly preserved for the same step sizes.

The plan of this work is as follows. The dynamics of the model (2) is studied in Section 2. The NSFD scheme is formulated and analyzed in Section 3. Numerical experiments are performed in Section 4. A note on qualitative study and numerical simulation of generalized versions of the proposed SEIR model is discussed in Section 5. Some remarks and open problems are discussed in the last section.

2. Dynamics of the generalized SEIR model

We first establish the positivity and boundedness of the model (2).

Lemma 1. *The set* $\Omega = \big\{(S, E, I, R) \in \mathbb{R}^4 | S, E, I, R \geq 0,\ S+E+I+R = 1\big\}$ *is a positively invariant set of the model* (2)*, that is,* $\big(S(t), E(t), I(t), R(t)\big) \in \Omega$ *for* $t > 0$ *if* $\big(S(0), E(0), I(0), R(0)\big) \in \Omega$*.*

Proof. First, it follows from the system (2) that

$$\begin{aligned} \dot{S}\big|_{S=0} &= \mu, \\ \dot{E}\big|_{E=0} &= \frac{\beta_0 SI}{\psi(I)}, \\ \dot{I}\big|_{I=0} &= \sigma E, \\ \dot{R}\big|_{R=0} &= \gamma I. \end{aligned}$$

Therefore, from [54, Theorem B.7] we conclude that $S(t), E(t), I(t), R(t) \geq 0$ for $t > 0$ whenever $S(0), E(0), I(0), R(0) \geq 0$.

Next, we introduce the *total population* $N(t) = S(t) + E(t) + I(t) + R(t)$ for $t \geq 0$. Then, from (2) we obtain

$$\dot{N} = \mu - \mu N, \qquad N(0) = 1, \tag{3}$$

which follows that $N(t) \equiv 1$ for $t \geq 0$. This is the desired conclusion and the proof is complete. □

As a direct consequence of the conservation property of the total population, Lemma 1, we can reduce the model (2) by one component, i.e. it is sufficient to consider the following *reduced model*

$$\begin{aligned} \dot{S} &= \mu - \frac{\beta_0 S I}{\psi(I)} - \mu S, \\ \dot{E} &= \frac{\beta_0 S I}{\psi(I)} - (\sigma + \mu)E, \\ \dot{I} &= \sigma E - (\gamma + \mu) I \end{aligned} \tag{4}$$

on its feasible set given by

$$\Omega^* = \left\{(S, I, E) \in \mathbb{R}^3 | S, E, I \geq 0,\ S + E + I \leq 1\right\}. \tag{5}$$

We now determine possible equilibrium points and calculate the basic reproduction number of the model (4).

Theorem 1 (Equilibria and basic reproduction number)**.**

(i) The model (4) *always possesses a disease-free equilibrium (DFE) point* $P_f = (S_f, E_f, I_f) = (1, 0, 0)$ *for all the values of the parameters.*

(ii) The basic reproduction number of the model (4) *can be computed as*

$$\mathcal{R}_0 = \frac{\beta_0 \sigma}{(\sigma + \mu)(\gamma + \mu)}.$$

(iii) The model (4) *has a unique disease-endemic equilibrium (DEE) point* $P_e = (S_e, E_e, I_e)$ *if and only if* $\mathcal{R}_0 > 1$*. Moreover, if existing* P_e *it is given by*

$$E_e = \frac{\gamma + \mu}{\sigma} I_e, \qquad S_e = \frac{(\sigma + \mu)(\gamma + \mu)\psi(I_e)}{\sigma \beta_0},$$

where I_e *is the unique positive solution of the equation*

$$F(I) = \mu - \mu \frac{(\sigma + \mu)(\gamma + \mu)\psi(I)}{\sigma} - \frac{(\sigma + \mu)(\gamma + \mu)}{\sigma} I = 0.$$

Proof. **Proof of Part (i)**. Let (S^*, E^*, I^*) be any equilibrium point. To determine the equilibrium points, we set the time derivatives in (4) to zero and thus consider the following system of algebraic equations

$$\begin{aligned} \mu - \frac{\beta_0 S^* I^*}{\psi(I^*)} - \mu S^* &= 0, \\ \frac{\beta_0 S^* I^*}{\psi(I^*)} - (\sigma + \mu) E^* &= 0, \\ \sigma E^* - (\gamma + \mu) I^* &= 0. \end{aligned} \tag{6}$$

The third equation of (6) yields

$$E^* = \frac{\gamma + \mu}{\sigma} I^*.$$

and inserting this in the second equation gives

$$I^* \Big[\frac{\beta_0 S^*}{\psi(I^*)} - \frac{(\sigma + \mu)(\gamma + \mu)}{\sigma} \Big] = 0. \tag{7}$$

Hence, the system (6) always possesses a trivial solution $(S_f, E_f, I_f) = (1, 0, 0)$, which corresponds to a DFE point of the model (4).

Proof of Part (ii). We apply the method of van den Driessche and Watmough [55] to compute the basic reproduction number $\mathcal{R}_0$. After reordering the variables in (4) as $x = (E, I, S)$, the DFE point is transformed to $x_f = (E_f, I_f, S_f)$ and (4) can be written in the matrix form

$$\dot{x} = \mathcal{F}(x) - \mathcal{V}(x),$$

where

$$\mathcal{F}(x) = \begin{pmatrix} \frac{\beta_0 S I}{\psi(I)} \\ 0 \\ \mu \end{pmatrix}, \qquad \mathcal{V}(x) = \begin{pmatrix} (\sigma + \mu) E, \\ -\sigma E + (\gamma + \mu) I \\ \frac{\beta_0 S I}{\psi(I)} + \mu S \end{pmatrix}.$$

Consequently,

$$D\mathcal{F}(x_f) = \begin{pmatrix} 0 & \beta_0 & 0 \\ 0 & 0 & 0 \\ 0 & 0 & 0 \end{pmatrix}, \qquad D\mathcal{V}(x_f) = \begin{pmatrix} \sigma + \mu & 0 & 0 \\ -\sigma & \gamma + \mu & 0 \\ 0 & 0 & \mu \end{pmatrix}.$$

Hence,

$$\mathcal{R}_0 = \rho(FV^{-1}) = \frac{\beta_0 \sigma}{(\sigma+\mu)(\gamma+\mu)}.$$

Proof of Part (iii). Note that a DEE point is a trivial solution of (6). From the first and second equations of (6), we obtain

$$\frac{\beta_0 S^* I^*}{\psi(I^*)} = (\sigma+\mu)E^* = \frac{(\sigma+\mu)(\gamma+\mu)}{\sigma} I^*. \tag{8}$$

On the other hand, it follows from (7) that

$$S^* = \frac{(\sigma+\mu)(\gamma+\mu)\psi(I^*)}{\sigma\beta_0}. \tag{9}$$

Combining (8) and (9) with the first equation of the reduced model (6) leads to an equation for I^*

$$F(I^*) = \mu - \mu\frac{(\sigma+\mu)(\gamma+\mu)\psi(I^*)}{\sigma} - \frac{(\sigma+\mu)(\gamma+\mu)}{\sigma} I^* = 0. \tag{10}$$

It is easy to verify that

$$\begin{aligned} F(0) &= \mu\Big(1 - \frac{1}{\mathcal{R}_0}\Big), \\ F(1) &< 0, \\ F'(I) &< 0. \end{aligned}$$

Therefore, if $\mathcal{R}_0 > 1$ then (10) has a unique positive solution $I_e \in (0,1)$, which corresponds to a unique DEE point. The proof is complete. □

We now analyze local and global asymptotic stability of the model (4).

Theorem 2 (Local asymptotic stability)**.** *smallskip*

(i) The DFE point P_f is locally asymptotically stable if $\mathcal{R}_0 < 1$ and unstable if $\mathcal{R}_0 > 1$.

(ii) The DEE point P_e is locally asymptotically stable if it exists ($\mathcal{R}_0 > 1$).

Proof. **Proof of Part (i).** The Jacobian matrix of the system (4) evaluated at P_f is given by

$$J(P_f) = \begin{pmatrix} -\mu & 0 & -\beta_0 \\ 0 & -(\sigma+\mu) & \beta_0 \\ 0 & \sigma & -(\gamma+\mu) \end{pmatrix}.$$

Hence, one of the three eigenvalues of $J(P_f)$ is $\lambda_1 = -\mu < 0$ and the two remaining eigenvalues are the ones of the sub-matrix

$$J^0(P_f) = \begin{pmatrix} -(\sigma+\mu) & \beta_0 \\ \sigma & -(\gamma+\mu) \end{pmatrix}.$$

It is clear that

$$\mathrm{Tr}(J^0) < 0, \quad \det(J^0) = (\sigma+\mu)(\gamma+\mu) - \beta_0\sigma = (\sigma+\mu)(\gamma+\mu)(1-\mathcal{R}_0) > 0.$$

Using the Routh-Hurwitz criterion [3, Theorem 4.4], we conclude that all eigenvalues of $J(P_f)$ are negative or have a negative real part. This confirms the local asymptotic stability of P_f. Otherwise, if $\mathcal{R}_0 > 1$, then $\det(J^0) < 0$, and thus P_f is unstable.

Proof of Part (ii). Note that P_f exists if and only if $\mathcal{R}_0 > 1$. For the sake of convenience, we denote $f(I) = \beta_0 I/\psi(I)$. Then, the Jacobian matrix of the system (4) evaluated at P_e is

$$J(P_e) = \begin{pmatrix} -(\mu + f(I_e)) & 0 & -S_e f'(I_e) \\ f(I_e) & -(\sigma+\mu) & S_e f'(I_e) \\ 0 & \sigma & -(\gamma+\mu) \end{pmatrix}.$$

Hence, the characteristic polynomial of $J(P_e)$ is given by

$$P_J(\lambda) = \lambda^3 + a_2\lambda^2 + a_1\lambda + a_0,$$

where

$$\begin{aligned} a_1 &= f(I_e) + \gamma + 3\mu + \sigma, \\ a_2 &= (\gamma+\mu)(f(I_e) + 2\mu + \sigma) + (f(I_e)+\mu)(\mu+\sigma) - S_e f'(I_e)\sigma, \\ a_3 &= (f(I_e)+\mu)(\gamma+\mu)(\mu+\sigma) - S f'(I_e)\mu\sigma. \end{aligned}$$

It follows from $f(I_e) > 0$ and $f'(I_e) < 0$ that

$$a_1 > 0, \quad a_2 > 0,$$
$$a_1a_2 - a_3 = f^2(I_e)\gamma + 2f^2(I_e)\mu + f^2(I_e)\sigma + f(I_e)\gamma^2 + 6f(I_e)\gamma\mu + 2f(I_e)\gamma\sigma$$
$$+ 8f(I_e)\mu^2 + 6f(I_e)\mu\sigma + f(I_e)\sigma^2 - S_ef'(I_e)f(I_e)\sigma + 2\gamma^2\mu + \gamma^2\sigma + 8\gamma\mu^2$$
$$+ 6\gamma\mu\sigma + \gamma\sigma^2 - S_ef'(I_e)\gamma\sigma + 8\mu^3 + 8\mu^2\sigma + 2\mu\sigma^2 - 2S_ef'(I_e)\mu\sigma - S_ef'(I_e)\sigma^2 > 0.$$

Therefore, we conclude from the Routh-Hurwitz criteria ([3, Theorem 4.4]) that P_f is locally asymptotically stable. The proof is thus complete. $\square$

Theorem 3 (Global asymptotic stability of the DFE point)**.** *The DFE point P_f is not only locally asymptotically stable but also globally asymptotically stable with respect to Ω^* when $\mathcal{R}_0 < 1$.*

Proof. Consider a candidate Lyapunov function $V\colon \Omega^* \to \mathbb{R}_+$ given by

$$V(S, E, I) = \Big(S - S_f - S_f \ln \frac{S}{S_f}\Big) + E + \frac{\mu + \sigma}{\sigma} I.$$

The derivative of V along with solutions of the system (4) is

$$\begin{aligned}
\frac{\mathrm{d}V}{\mathrm{d}t} &= \frac{\mathrm{d}V}{\mathrm{d}S}\frac{\mathrm{d}S}{\mathrm{d}t} + \frac{\mathrm{d}V}{\mathrm{d}E}\frac{\mathrm{d}E}{\mathrm{d}t} + \frac{\mathrm{d}V}{\mathrm{d}I}\frac{\mathrm{d}I}{\mathrm{d}t} \\
&= \Big(\mu - \frac{\beta_0 SI}{\psi(I)} - \mu S\Big)\frac{S - S_f}{S} + \Big[\frac{\beta_0 SI}{\psi(I)} - (\sigma + \mu)E\Big] \\
&\quad + \frac{\sigma + \mu}{\sigma}\big[\sigma E - (\gamma + \mu)I\big] \\
&= -\frac{\mu}{S}(S - S_f)^2 + I\Big[\frac{\beta_0}{\psi(I)} - \frac{(\sigma + \mu)(\gamma + \mu)}{\sigma}\Big] \\
&\le -\frac{\mu}{S}(S - S_f)^2 + I\Big[\beta_0 - \frac{(\sigma + \mu)(\gamma + \mu)}{\sigma}\Big] \\
&\le -\frac{\mu}{S}(S - S_f)^2 + \frac{(\sigma + \mu)(\gamma + \mu)}{\sigma}(\mathcal{R}_0 - 1)I.
\end{aligned}$$

Since $\mathcal{R}_0 < 1$, $\mathrm{d}V/\mathrm{d}t \le 0$ for all $S, E, I \ge 0$ and $\mathrm{d}V/\mathrm{d}t = 0$ if and only if $S = S_f$ and $I = I_f$. Consequently, it follows from LaSalle's invariance principle [35] that P_e is globally asymptotically stable. The proof is thus complete. $\square$

Remark 2. *The Lyapunov function in the proof of Theorem 3 is different from the one used in [38, Propostion 2.1].*

Li and Muldowney [39] proposed a general criterion for the orbital stability of periodic orbits associated with higher-dimensional nonlinear autonomous systems as well as with the theory of competing systems of differential equations to study the global stability of a SEIR model similar to (4). Thus, by applying this approach [39], we can obtain the global asymptotic stability of P_e.

Proposition 1. *The DEE point P_e is not only locally asymptotically stable but also globally asymptotically stable with respect to the interior of Ω^* whenever $\mathcal{R}_0 > 1$.*

Remark 3. *In [53], only the local asymptotic stability of the DFE point of the model* (1) *was studied. Therefore, the stability analysis of the model* (2) *is an important improvement of the results constructed in [53]. On the other hand, the global stability of the DFE points of the models* (1) *and* (2) *is very important because it means that infectious diseases can be eradicated (when $\mathcal{R}_0 < 1$), and thus some mitigation and prevention measures can be proposed.*

3. Construction of a dynamically consistent NSFD model

Our main goal in this section is to formulate an NSFD model that is dynamically consistent with the model (2). To this end, we first consider the model (2) on a time interval $[0, T]$ and partition this interval by a uniform mesh

$$0 = t_0 < t_1 < \cdots < t_{N-1} < T_N = T,$$

where $t_n - t_{n-1} = \Delta t$ for $n \geq 1$. Let $\big(S_n, E_n, I_n, R_n\big)$ denote the intended approximation for $\big(S(t_n), E(t_n), I(t_n), R(t_n)\big)$. Using Mickens' methodology [43, 44, 45], we approximate the differential equation model (2) with a difference equation model as follows:

$$\begin{aligned} \dot{S}(t_n) &\approx \frac{S_{n+1} - S_n}{\phi(\Delta t)}, \qquad \dot{E}(t_n) \approx \frac{E_{n+1} - E_n}{\phi(\Delta t)}, \\ \dot{I}(t_n) &\approx \frac{I_{n+1} - I_n}{\phi(\Delta t)}, \qquad \dot{R}(t_n) \approx \frac{R_{n+1} - R_n}{\phi(\Delta t)}, \end{aligned} \tag{11}$$

and

$$\begin{aligned}
\mu - \frac{\beta_0 S(t_n) I(t_n)}{\psi(I_n)} - \mu S(t_n) &\approx \mu - \frac{\beta_0 S_{n+1} I_n}{\psi(I_n)} - \mu S_{n+1}, \\
\frac{\beta_0 S(t_n) I(t_n)}{\psi(I_n)} - (\sigma + \mu) E(t_n) &\approx \frac{\beta_0 S_{n+1} I_n}{\psi(I_n)} - (\sigma + \mu) E_{n+1}, \\
\sigma E(t_n) - (\gamma + \mu) I(t_n) &\approx \sigma E_{n+1} - (\gamma + \mu) I_{n+1}, \\
\gamma I(t_n) - \mu R(t_n) &\approx \gamma I_{n+1} - \mu R_{n+1},
\end{aligned} \tag{12}$$

where $\phi(\Delta t) = \Delta t + \mathcal{O}(\Delta t^2)$ as $\Delta t \to 0$, which is called the *nonstandard denominator function*. The approximations (11) and (12) lead to the following NSFD scheme

$$\begin{aligned}
\frac{S_{n+1} - S_n}{\phi(\Delta t)} &= \mu - \frac{\beta_0 S_{n+1} I_n}{\psi(I_n)} - \mu S_{n+1}, \\
\frac{E_{n+1} - E_n}{\phi(\Delta t)} &= \frac{\beta_0 S_{n+1} I_n}{\psi(I_n)} - (\sigma + \mu) E_{n+1}, \\
\frac{I_{n+1} - I_n}{\phi(\Delta t)} &= \sigma E_{n+1} - (\gamma + \mu) I_{n+1}, \\
\frac{R_{n+1} - R_n}{\phi(\Delta t)} &= \gamma I_{n+1} - \mu R_{n+1}.
\end{aligned} \tag{13}$$

Our task is to analyze dynamics of the NSFD model (13). We will show that (13) shares typical properties of the underlying continuous model (2) on the discrete level and independently of the time step size Δt.

Lemma 2. *The set* $\Omega = \big\{(S, E, I, R) \in \mathbb{R}^4 | S, E, I, R \geq 0,\ S+E+I+R = 1\big\}$ *is a positively invariant set of the NSFD model* (13)*, i.e.,* $\big(S_n, E_n, I_n, R_n\big) \in \Omega$ *for* $n \geq 1$ *if* $\big(S(0), E(0), I(0), R(0)\big) \in \Omega$*.*

Proof. The lemma is proved by mathematical induction. First, it is straightforward to convert the NSFD scheme (13) into a a form that can be evaluated sequentially in an explicit way:

$$
\begin{aligned}
S_{n+1} &= \frac{S_n + \phi(\Delta t)\mu}{1 + \phi(\Delta t)\frac{\beta_0 I_n}{\psi(I_n)} + \phi(\Delta t)\mu}, \\
E_{n+1} &= \frac{E_n + \phi(\Delta t)\frac{\beta_0 I_n S_{n+1}}{\psi(I_n)}}{1 + \phi(\Delta t)(\sigma + \mu)}, \\
I_{n+1} &= \frac{I_n + \phi(\Delta t)\sigma E_{n+1}}{1 + \phi(\Delta t)(\gamma + \mu)}, \\
R_{n+1} &= \frac{R_n + \phi(\Delta t)\gamma I_{n+1}}{1 + \phi(\Delta t)\mu},
\end{aligned}
\tag{14}
$$

which implies that $S_{n+1}, E_{n+1}, I_{n+1}, R_{n+1} \geq 0$ if $S_n, E_n, I_n, R_n \geq 0$.

Next, setting $N_n = S_n + E_N + I_n + R_n$ for $n \geq 0$ we obtain from (13)

$$
\frac{N_{n+1} - N_n}{\phi(\Delta t)} = \mu - \mu N_{n+1}, \quad N_0 = 1, \tag{15}
$$

cf. (3), or equivalently

$$
N_{n+1} = \frac{N_n + \phi(\Delta t)\mu}{1 + \phi(\Delta t)\mu}, \quad N_0 = 1.
$$

It is easy to verify that $\{N_n\}_{n\in\mathbb{N}}$ with $N_n \equiv 1$ is the unique solution of this difference equation (15). The proof is complete. □

As a direct consequence of Lemma 2, it suffices to consider the following reduced discrete model of (13).

$$
\begin{aligned}
\frac{S_{n+1} - S_n}{\phi(\Delta t)} &= \mu - \frac{\beta_0 S_{n+1} I_n}{\psi(I_n)} - \mu S_{n+1}, \\
\frac{E_{n+1} - E_n}{\phi(\Delta t)} &= \frac{\beta_0 S_{n+1} I_n}{\psi(I_n)} - (\sigma + \mu)E_{n+1}, \\
\frac{I_{n+1} - I_n}{\phi(\Delta t)} &= \sigma E_{n+1} - (\gamma + \mu)I_{n+1}
\end{aligned}
\tag{16}
$$

defined on the set Ω^* given by (5).

We now compute the basic reproduction number $\mathcal{R}_0$ for the discrete model (16) using the next generation matrix approach [4]. It is easy to verify that (16) always has a unique DFE point $P_f^* = (S_f^*, E_f^*, I_f^*) = (1, 0, 0)$ for all values of the parameters. If we reorder the variables in (16) as (E_n, I_n, S_n), then the DFE point is transformed into $(0, 0, 1)$. The Jacobian matrix of (16) at P_f^* reads

$$J(P_f^*) = \begin{pmatrix} \frac{1}{1+\phi(\sigma+\mu)} & \frac{\phi\beta_0}{1+\phi(\sigma+\mu)} & 0 \\ \frac{\phi\sigma}{\left[1+\phi(\gamma+\mu)\right]\left[1+\phi(\sigma+\mu)\right]} & \frac{1}{1+\phi(\gamma+\mu)} + \frac{\phi\sigma}{1+\phi(\gamma+\mu)} & 0 \\ 0 & \frac{\phi\beta_0}{1+\phi\mu} & \frac{1}{1+\phi\mu} \end{pmatrix}.$$

Following the method of Allen and van den Driessche [4] we write $J(P_f^*)$ in the form

$$J(P_f^*) = \begin{pmatrix} F+T & 0 \\ A & C \end{pmatrix},$$

where

$$F = \begin{pmatrix} 0 & 0 \\ \frac{\phi\sigma}{\left[1+\phi(\gamma+\mu)\right]\left[1+\phi(\sigma+\mu)\right]} & \frac{\phi\sigma}{1+\phi(\gamma+\mu)} \end{pmatrix}, \qquad A = 0,$$

$$T = \begin{pmatrix} \frac{1}{1+\phi(\sigma+\mu)} & \frac{\phi\beta_0}{1+\phi(\sigma+\mu)} \\ 0 & \frac{1}{1+\phi(\gamma+\mu)} \end{pmatrix}, \qquad C = \frac{1}{1+\phi\mu}.$$

It is easy to verify that F and T are non-negative, $F+T$ is irreducible, and the matrices C and T satisfy

$$\rho(C) < 1, \qquad \rho(T) < 1.$$

Therefore, the basic reproduction number $\mathcal{R}_0$ of the discrete model (16) can be computed by the spectral radius

$$\mathcal{R}_0 = \rho\big(F(I-T)^{-1}\big) = \frac{\beta_0\sigma}{(\sigma+\mu)(\gamma+\mu)}.$$

This means that the basic reproduction numbers of (16) and (4) are identical.

The following assertion is a direct consequence of Theorem 2.1 in [4].

Corollary 1. *The DFE point P_f^* of the NSFD scheme* (16) *is locally asymptotically stable if $\mathcal{R}_0 < 1$ and unstable if $\mathcal{R}_0 > 1$.*

The global asymptotic stability of the DFE point P_f^* of (16) is established in the following theorem.

Theorem 4 (Global stability of the DFE point)**.** *Assume that the denominator function $\phi(\Delta t)$ satisfies*

$$\phi(\Delta t) < \frac{\sigma+\mu}{\beta_0\sigma}(1-\mathcal{R}_0) \tag{17}$$

for all $\Delta t > 0$. Then, the DFE point P_f^* of the NSFD scheme (16) *is not only locally asymptotically stable but also globally asymptotically stable if $\mathcal{R}_0 < 1$.*

Proof. Consider a candidate Lyapunov function $L\colon \Omega^* \to \mathbb{R}_+$ defined by

$$L(S,E,I) = E + \frac{\sigma+\mu}{\sigma}I. \tag{18}$$

Note that $0 \le S_n \le 1$ for $n \ge 0$. On the other hand, it follows from the properties (H1)–(H3) of the function ψ that $\psi(I) \ge 1$ for $I \ge 0$. Thus, from the last two equations of the system (16) we obtain

$$\begin{aligned}
\frac{E_{n+1}-E_n}{\phi(\Delta t)} &= \frac{\beta_0 S_{n+1} I_n}{\psi(I_n)} - (\sigma+\mu)E_{n+1} \le \beta_0 I_n - (\sigma+\mu)E_{n+1},\\
\frac{I_{n+1}-I_n}{\phi(\Delta t)} &= \sigma E_{n+1} - (\gamma+\mu)I_{n+1}\\
&= \sigma E_{n+1} - (\gamma+\mu)\frac{I_n + \phi(\Delta t)\sigma E_{n+1}}{1+\phi(\Delta t)(\gamma+\mu)}\\
&\le \sigma E_{n+1} - \frac{(\gamma+\mu)I_n}{1+\phi(\Delta t)(\gamma+\mu)}.
\end{aligned} \tag{19}$$

Here we used the third equation of the system (14) to obtain the final estimate of (19). We derive from (18) and (19) that

$$\begin{aligned}
\Delta L(S_n,E_n,I_n) &= L(S_{n+1},E_{n+1},I_{n+1}) - L(S_n,E_n,I_n)\\
&= (E_{n+1}-E_n) + \frac{\sigma+\mu}{\sigma}(I_{n+1}-I_n)\\
&\le \big[\beta_0 I_n - (\sigma+\mu)E_{n+1}\big] + \frac{\sigma+\mu}{\sigma}\Big[\sigma E_{n+1} - \frac{(\gamma+\mu)I_n}{1+\phi(\Delta t)(\gamma+\mu)}\Big]\\
&= \Big[\beta_0 - \frac{\sigma+\mu}{\sigma}\frac{\gamma+\mu}{1+\phi(\Delta t)(\gamma+\mu)}\Big]I_n\\
&= \frac{(\sigma+\mu)(\gamma+\mu)(\mathcal{R}_0-1) + \phi(\Delta t)\beta_0\sigma(\gamma+\mu)}{\sigma+\phi(\Delta t)\sigma(\gamma+\mu)}I_n.
\end{aligned}$$

Since $\phi(\Delta t)$ satisfies the condition (17), $\Delta L(S_n, E_n, I_n) \leq 0$ and $\Delta L(S_n, E_n, I_n) = 0$ if and only if $E_n = I_n = 0$. Thus, by applying LaSalle's invariance principle [21, 36] we conclude that

$$\lim_{n\to\infty}(S_n, E_n, I_n) = (1, 0, 0).$$

Consequently, the global asymptotic stability of the DFE point is achieved. $\square$

Remark 4. *It is possible to use the Lyapunov function candidate* (18) *to determine the global asymptotic stability of the DFE point of the continuous model* (2)*. This means that the NSFD scheme can preserve the Lyapunov function for the model* (2)*.*

Similar to Theorem 1, it is easy to prove that the NSFD model (16) has a unique DEE point $P_e^* = (S_e^*, E_e^*, I_e^*)$ if and only if $\mathcal{R}_0 > 1$, where $P_e^* = P_e$. Using the approach proposed in [27], the local asymptotic stability of P_e^* is determined as follows.

Proposition 2. *Let us assume that $\mathcal{R}_0 > 1$. Then there is a positive number $\phi^* > 0$ which depends only on the values of the parameters of the model* (2) *and serves as a stability threshold for the NSFD model* (16)*, i.e. P_e^* is locally asymptotically stable if*

$$\phi(\Delta t) < \phi^* \quad \text{for all} \quad \Delta t > 0.$$

Remark 5. *Similar to Theorem 3 in [27], we can verify that the NSFD scheme* (16) *is convergent of order 1.*

The results developed in this section lead to the following theorem.

Theorem 5. *The NSFD scheme* (13) *is dynamically consistent with respect to the positivity, boundedness, and asymptotic stability of the SEIR model* (2) *if*

$$\phi(\Delta t) < \tau^* \quad \text{for all} \quad \Delta t > 0,$$

where

$$\tau^* = \begin{cases} \infty & \text{if} \quad \mathcal{R}_0 < 1, \\ \phi^* & \text{if} \quad \mathcal{R}_0 > 1. \end{cases}$$

Furthermore, if $\mathcal{R}_0 < 1$ *and*

$$\phi(\Delta t) < \Delta t^*_{GAS} := \frac{\sigma + \mu}{\beta_0 \sigma}(1 - \mathcal{R}_0) \quad \textit{for all} \quad \Delta t > 0,$$

then the NSFD scheme (13) *is also dynamically consistent with respect to the global asymptotic stability of the DFE point of the model* (2)*.*

Remark 6.

(i) Using the approaches used in [12, 30], we can conclude that the NSFD scheme (13) *is convergent of order 1.*

(ii) In the numerical experiments performed in the next section, we will use the following denominator function for the NSFD scheme (16)

$$\phi(\Delta t) = \frac{1 - e^{\tau \Delta t}}{\tau}, \qquad \tau > \max\left\{\frac{1}{\tau^*}, \frac{1}{\Delta t^*_{GAS}}\right\}.$$

(iii) The approach used to construct the NSFD scheme (13) *can be extended to obtain dynamically consistent NSFD schemes for the SEIR models considered in [38, 59].*

4. Numerical experiments

In this section, we report some numerical examples to support the theoretical findings. As we will see later, these examples support the results constructed in Sections 2 and 3. All numerical examples use the function $\psi(I) = 1 + \alpha I^2$ (see [53]) and the following data.

Example 1 (Numerical dynamics of the NSFD scheme and standard Runge-Kutta schemes)**.** *We now compare the NSFD scheme* (16) *with two well-known standard Runge-Kutta schemes, namely the Euler scheme and the second-order Runge-Kutta (RK2) scheme (see [6]). Here, for the NSFD scheme, we have* $\Delta t^*_{GAS} = 4$*; therefore, a suitable denominator function is*

$$\phi(\Delta t) = \frac{1 - e^{-0.25 \Delta t}}{0.25}.$$

The numerical solutions obtained by the above methods for the initial data $(S(0), E(0), I(0)) = (0.7, 0.2, 0.1)$ *are shown in Figures 1-9. From these figures, it can be seen that the Euler and RK2 methods produce not only negative* *but also unstable approximations for the step size $\Delta t = 1.5$. This destroys the dynamic properties of the SEIR model. Conversely, the NSFD scheme correctly preserves the dynamics of the SEIR model for the same step size. Even when using a larger step size, namely $\Delta t = 2.0$, the dynamics of the SEIR model is preserved by the NSFD scheme (see Figure 9). This is evidence for the claim that the NSFD scheme preserves the dynamics of the SEIR model for all finite step sizes.*

Example 2 (Dynamics of the SEIR model when $\mathcal{R}_0 < 1$)**.** *We now consider the dynamics and global asymptotic stability of the SEIR model by numerical solutions using the parameters in Case 2 in Table 1. In this case, it is easy to obtain that $\Delta t^*_{GAS} = 3.3824$; therefore, we can choose a suitable denominator function given by*

$$\phi(\Delta t) = \frac{1 - e^{-0.30\Delta t}}{0.30}.$$

Figures 10-12 outline numerical solutions obtained with the NSFD scheme over the time interval $[0, 150]$ with different values of the step size. It is clear that the DFE point is globally asymptotically stable when $\mathcal{R}_0 < 1$. Moreover, the numerical dynamics of the NSFD scheme does not depend on the values of the chosen step size.

Example 3 (Dynamics of the SEIR model when $\mathcal{R}_0 > 1$)**.** *We now consider the dynamics and global asymptotic stability of the SEIR model through numerical solutions using the parameters in Case 3 in Table 1. Figures 13-15 show numerical solutions obtained using the NSFD scheme over the time interval $[0, 150]$ with different values for the step size. Here the denominator function is given by $\phi(\Delta t) = 1 - e^{-\Delta t}$. It is clear that the DEE point is not only locally asymptotically stable, but also globally asymptotically stable when $\mathcal{R}_0 > 1$. Moreover, similar to Example 2, the numerical dynamics of the NSFD scheme does not depend on the values of the chosen step size. From this example, it can be assumed that the NSFD scheme also preserves the global asymptotic stability of the model (2).*

Table 1: The parameters used in the numerical simulations

Case	μ	γ	σ	β_0	α	Source	$\mathcal{R}_0$	GAS equilibrium point
1	0.2	0.8	0.8	0.25	0.75	Assumed	0.2	$P_f = (1, 0, 0)$
2	0.1	1/7	1/5	0.2	0.75	[53]	0.5490	$P_f = (1, 0, 0)$
3	0.1	1/7	1/5	0.75	0.5	[53]	2.0588	$P_e = (0.4904, 0.1699, 0.1399)$

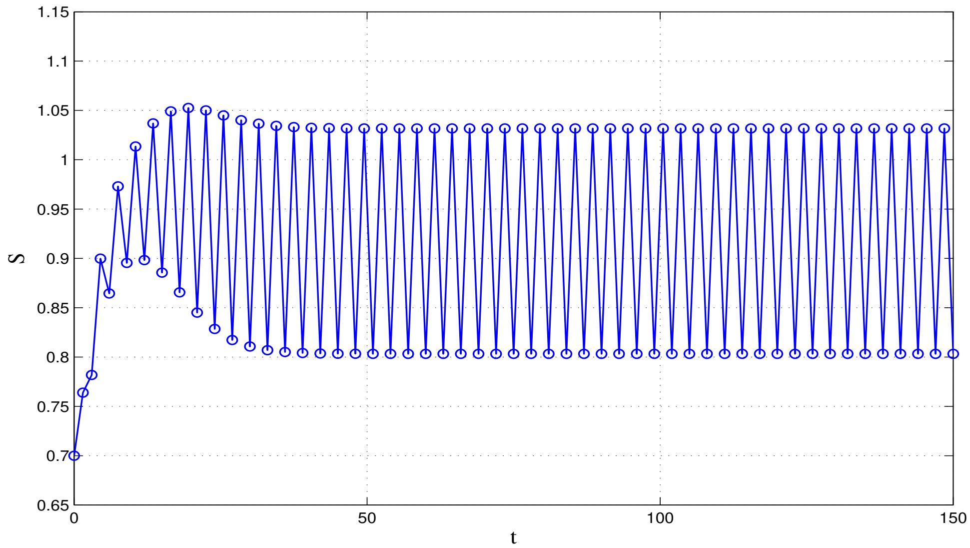

Figure 1: The S-component generated by the Euler scheme in Case 1 with $\Delta t = 1.5$.

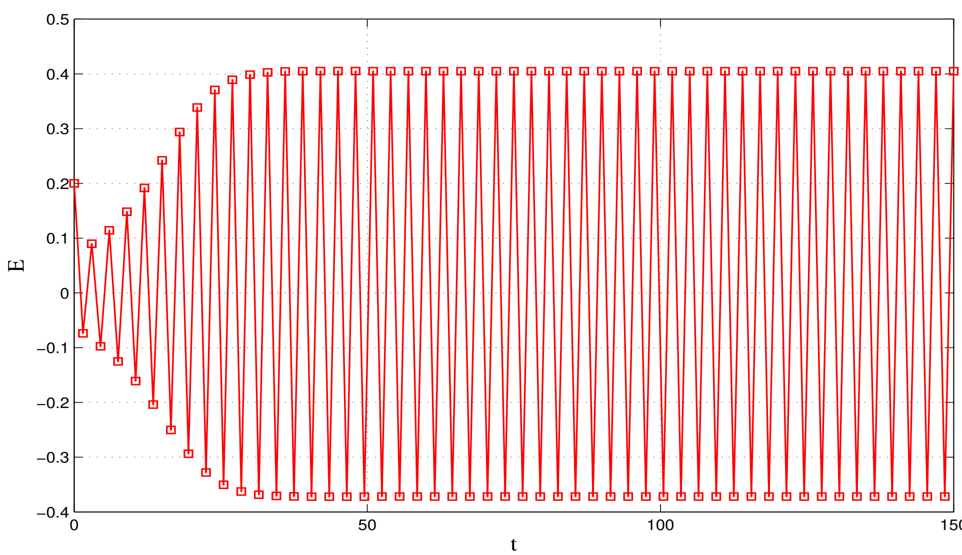

Figure 2: The E-component generated by the Euler scheme in Case 1 with $\Delta t = 1.5$.

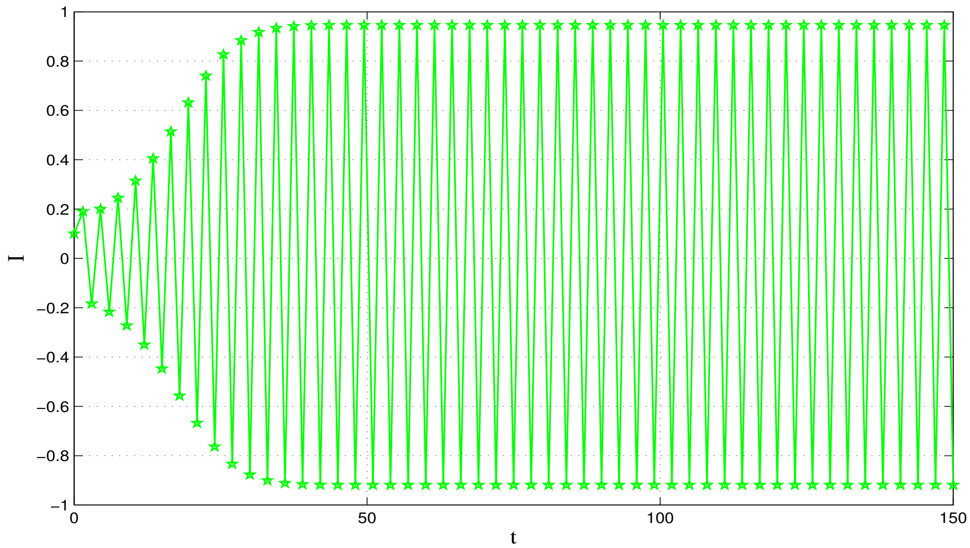

Figure 3: The I-component generated by the Euler scheme in Case 1 with $\Delta t = 1.5$.

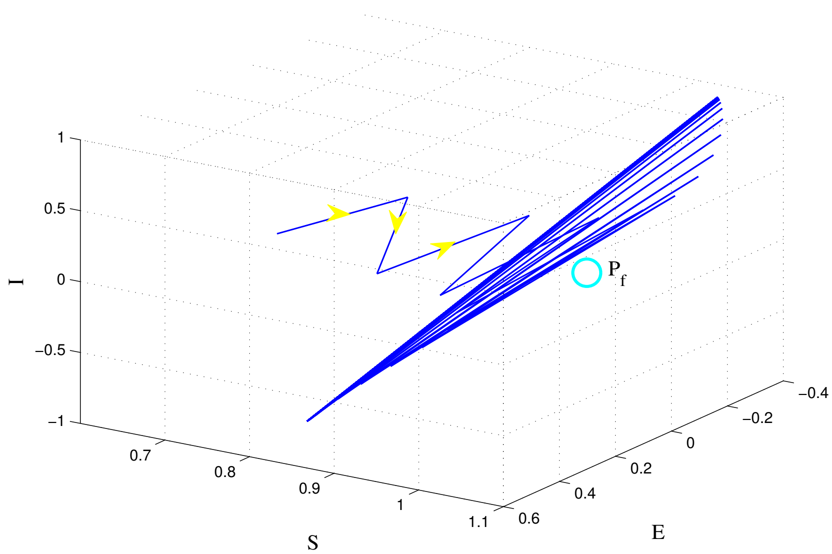

Figure 4: The phase space generated by the Euler scheme in Case 1 with $\Delta t = 1.5$.

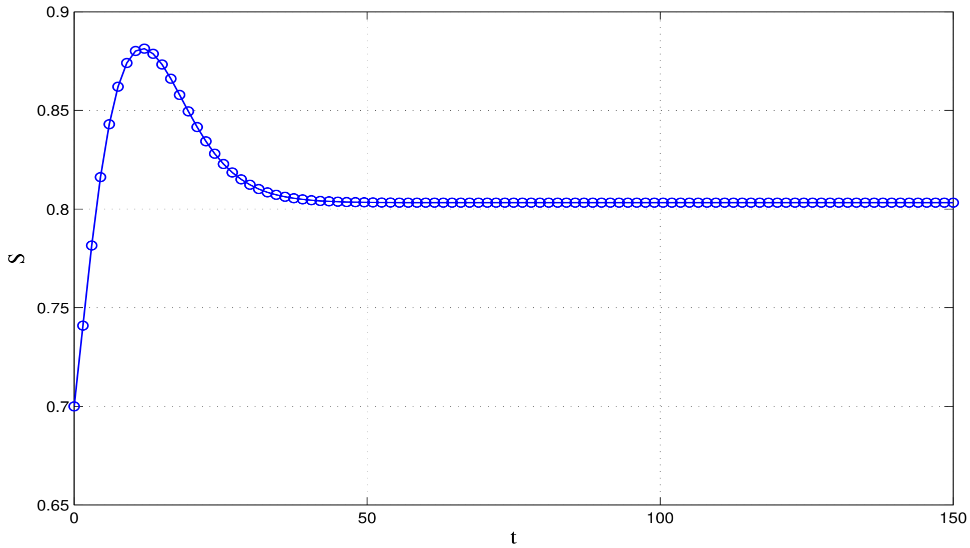

Figure 5: The S-component generated by the RK2 scheme in Case 1 with $\Delta t = 1.5$.

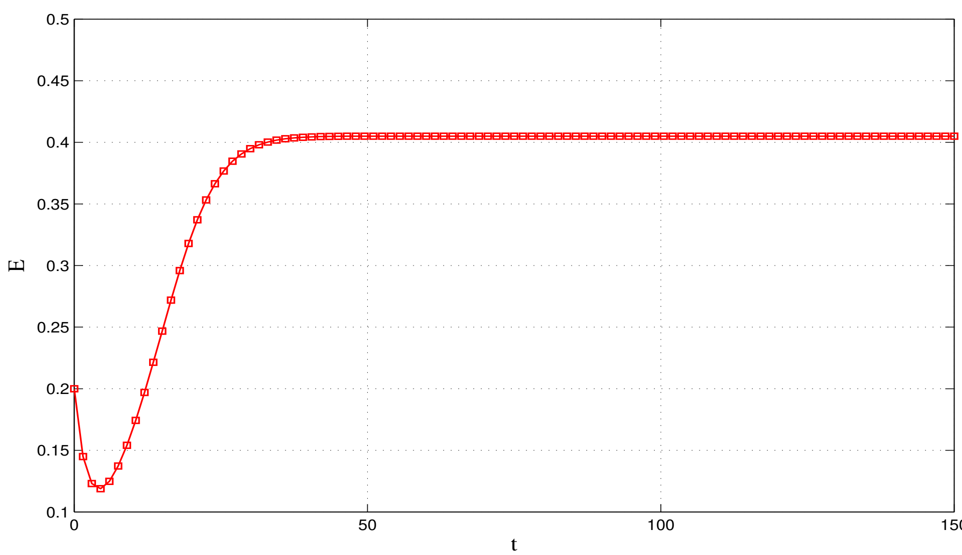

Figure 6: The E-component generated by the RK2 scheme in Case 1 with $\Delta t = 1.5$.

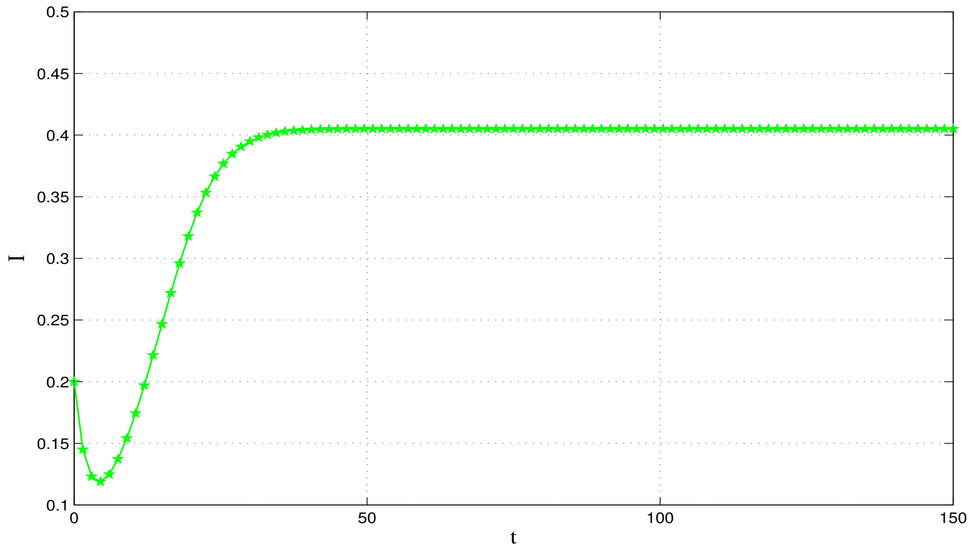

Figure 7: The I-component generated by the RK2 scheme in Case 1 with $\Delta t = 1.5$.

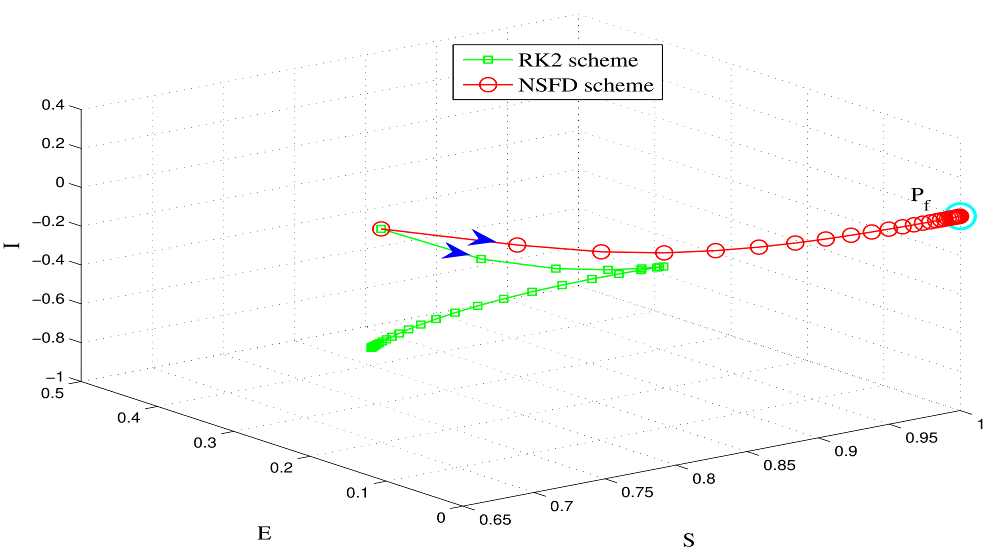

Figure 8: The phase spaces generated by the RK2 and NSFD schemes in Case 1 with $\Delta t = 1.5$.

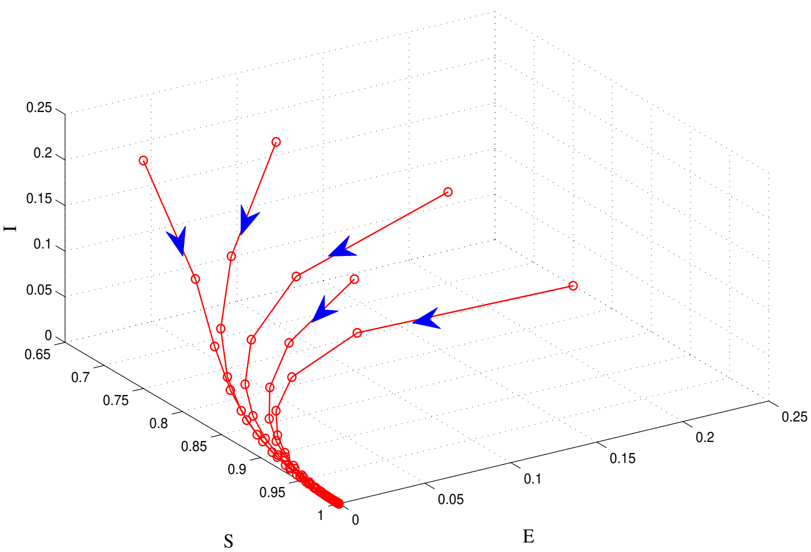

Figure 9: The phase spaces generated by the NSFD scheme in Case 1 with $\Delta t = 2.0$.

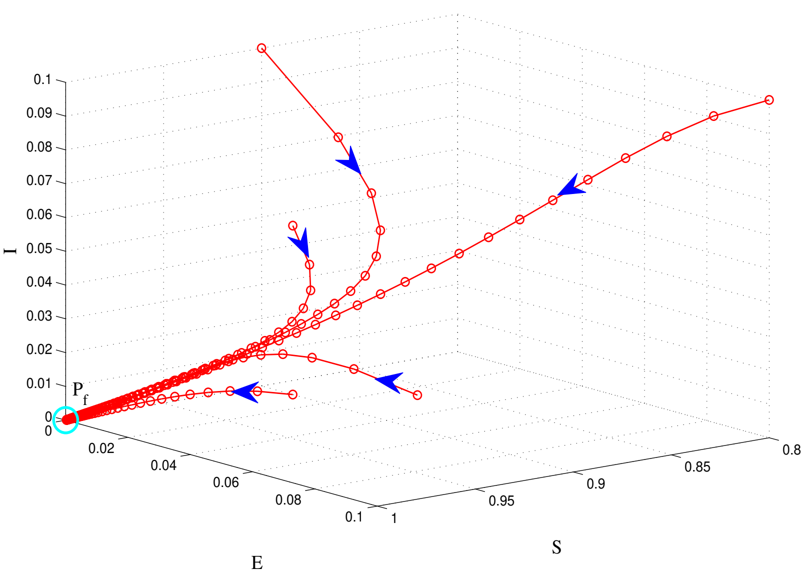

Figure 10: The phase spaces generated by the NSFD scheme in Case 2 with $\Delta t = 2.0$.

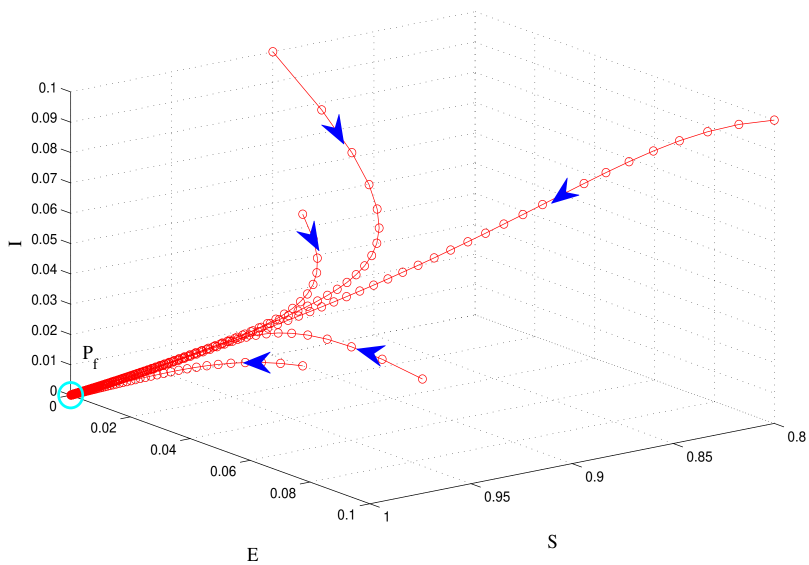

Figure 11: The phase spaces generated by the NSFD scheme in Case 2 with $\Delta t = 1.0$.

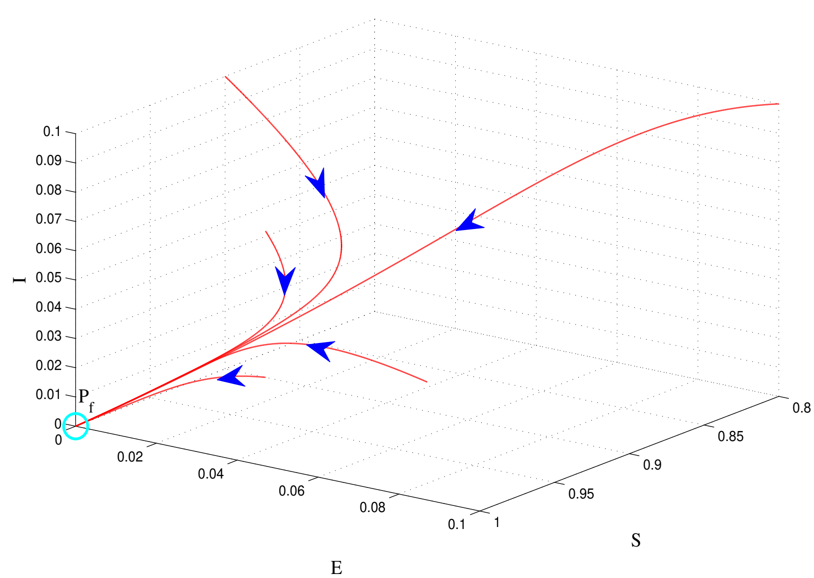

Figure 12: The phase spaces generated by the NSFD scheme in Case 2 with $\Delta t = 10^{-3}$.

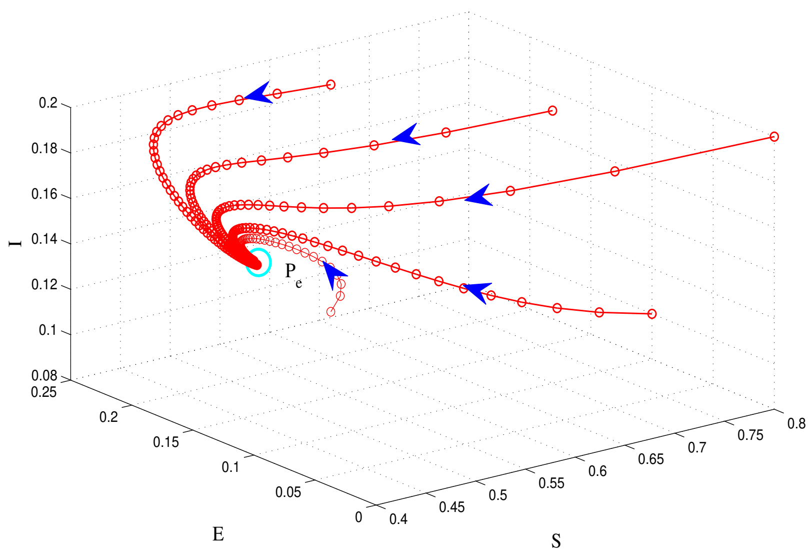

Figure 13: The phase spaces generated by the NSFD scheme in Case 3 with $\Delta t = 2.0$.

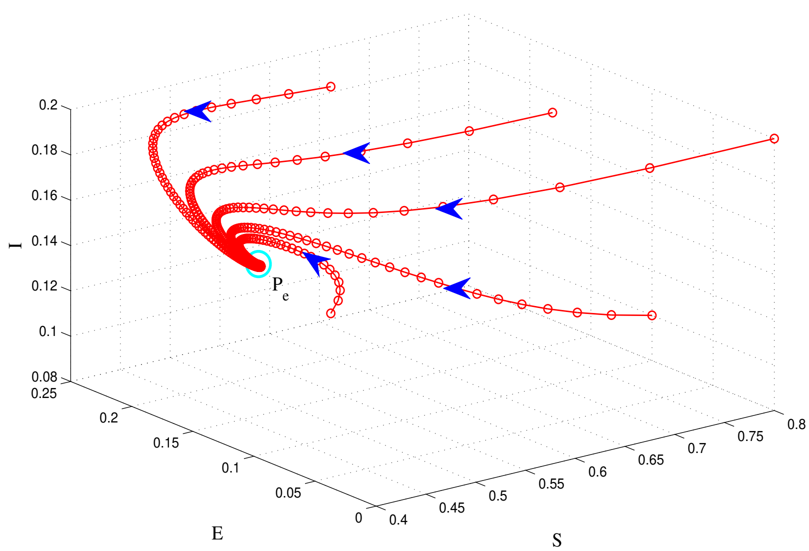

Figure 14: The phase spaces generated by the NSFD scheme in Case 3 with $\Delta t = 1.0$.

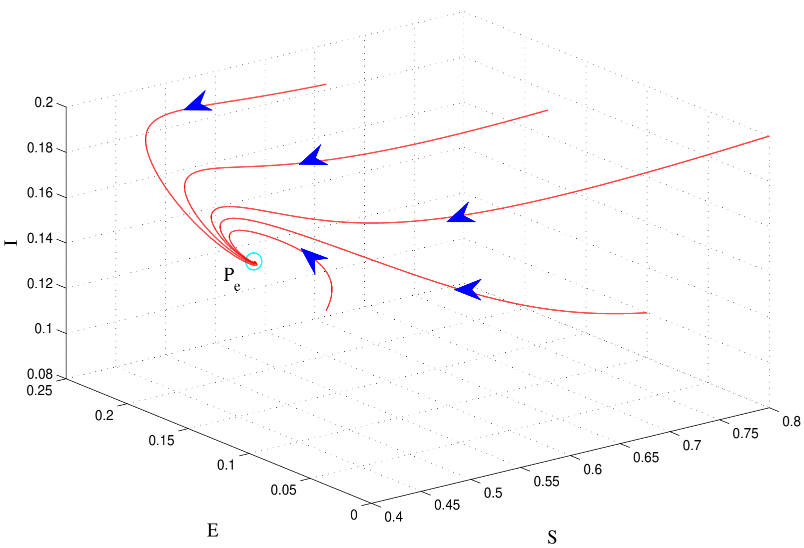

Figure 15: The phase spaces generated by the NSFD scheme in Case 3 with $\Delta t = 10^{-3}$.

5. A note on the qualitative investigation and numerical simulation of generalized versions of the proposed SEIR model

In recent years, mathematical models based on fractional-order differential equations have been intensively studied and widely used to explore complex systems arising in real-world applications due to their accuracy superior compared to integer-order models (ODE) models (see, for example, [5, 10, 24, 56]). Following this approach, we now consider the model (2) in the context of the Caputo fractional derivative

$$\begin{aligned}
{}^{C}D_{0+}^{q}S(t) &= \mu^q - \frac{\beta_0^q SI}{\psi(I)} - \mu^q S,\\
{}^{C}D_{0+}^{q}E(t) &= \frac{\beta_0^q SI}{\psi(I)} - (\sigma^q + \mu^q)E,\\
{}^{C}D_{0+}^{q}I(t) &= \sigma^q E - (\gamma^q + \mu^q)I,\\
{}^{C}D_{0+}^{q}E(t) &= \gamma^q I - \mu^q R,
\end{aligned} \tag{20}$$

where ${}_0^C D_t^q f(t)$ and with $q \in (0, 1)$ stands for the Caputo fractional derivative of the function $f(t)$ and is defined by [9, 18, 32, 52]

$$ {}^C D_{0+}^q f(t) = \frac{1}{\Gamma(1-q)} \int_a^t \frac{f'(\tau)}{(t-\tau)^q} \, d\tau. $$

When $q = 1$, the model (20) is reduced to the integer-order model (2); thus, it is a generalization of (2). On the other hand, the appearance of the fractional order α makes the model more flexible and can include time memory effects to the model. This is very useful in the study of the parameter estimation problem.

Applying Lyapunov stability theory for fractional dynamical systems [1, 19, 40, 41, 56, 57] and the arguments used in Section 2, we obtain the following results for the dynamics of the fractional-order model (20)

Theorem 6. *The following assertions are true for the fractional-order model* (20)*:*

(i) The system (20) *admits the set* $\Omega = \{(S, E, I, R) \in \mathbb{R}^4 | S, E, I, R \geq 0,\ S + E + I + R = 1\}$ *as a positively invariant set.*

(ii) The model (20) *always possesses a disease-free equilibrium (DFE) point* $P_f^F = (1, 0, 0, 0)$ *for all the values of the parameters. Meanwhile, a unique disease-endemic equilibrium (DEE) point* $P_e^F = (S_e^F, E_e^F, I_e^F, R_e^F)$ *exists if and only if* $\mathcal{R}_0 > 1$*, where*

$$ \mathcal{R}_0^q = \frac{\beta_0^q \sigma^q}{(\sigma^q + \mu^q)(\gamma^q + \mu^q)}. $$

can be considered as a threshold value of the model (20) *and* P_e^F *is determined similarly to the DFE point of the integer-order model* (2)*.*

(iii) The DFE point P_f^F *is not only locally asymptotically stable but also globally asymptotically stable with respect to* Ω *if* $\mathcal{R}_0^q < 1$*.*

(iv) The DEE point P_e^F *is locally asymptotically stable if* $\mathcal{R}_0^q > 1$*.*

Since all solutions of the model (20) are positive, we now introduce a positivity-preserving NSFD scheme for the fractional-order model (20). A general family of NSFD schemes for fractional-order models can be found in [13]. Using the Grunwald-Letnikov definition for the Caputo fractional derivative (see [52]), we obtain

$$ {}^{C}D^{q}_{0+}z(t) = \lim_{\Delta t \to 0} \frac{1}{\Delta t^{q}} \Delta^{q}_{\Delta t} z(t), \tag{21} $$

where

$$ \begin{aligned} \frac{1}{\Delta t^{q}} \Delta^{q}_{\Delta t} z(t) &= \frac{1}{\Delta t^{q}} \Big(z(\tau_{n+1}) - \sum_{\nu=1}^{n+1} c^{q}_{\nu} z(\tau_{n+1-\nu}) \Big), \\ c^{q}_{\nu} &= (-1)^{q-1} \binom{q}{\nu}, \\ \binom{q}{\nu} &:= \frac{q(q-1)(q-2)\dots(q-\nu+1)}{\nu!}. \end{aligned} $$

Next, by combining (21) with the non-local approximation (12), we obtain the following NSFD scheme

$$ \begin{aligned} \frac{1}{\Delta t^{q}} \Big(S_{n+1} - \sum_{\nu=1}^{n+1} c^{q}_{\nu} S_{n+1-\nu} \Big) &= \mu^{q} - \frac{\beta^{q}_{0} S_{n+1} I_{n}}{\psi(I_{n})} - \mu^{q} S_{n+1}, \\ \frac{1}{\Delta t^{q}} \Big(E_{n+1} - \sum_{\nu=1}^{n+1} c^{q}_{\nu} E_{n+1-\nu} \Big) &= \frac{\beta^{q}_{0} S_{n+1} I_{n}}{\psi(I_{n})} - (\sigma^{q} + \mu^{q}) E_{n+1}, \\ \frac{1}{\Delta t^{q}} \Big(I_{n+1} - \sum_{\nu=1}^{n+1} c^{q}_{\nu} I_{n+1-\nu} \Big) &= \sigma^{q} E_{n+1} - (\gamma^{q} + \mu^{q}) I_{n+1}, \\ \frac{1}{\Delta t^{q}} \Big(R_{n+1} - \sum_{\nu=1}^{n+1} c^{q}_{\nu} R_{n+1-\nu} \Big) &= \gamma^{q} I_{n+1} - \mu^{q} R_{n+1}, \end{aligned} \tag{22} $$

where (S_n, E_n, I_n, R_n) is the intended approximation for $(S(t_n), E(t_n), I(t_n), R(t_n))$ $(n \geq 1)$. Then it is straightforward to prove the following result about the positivity of the NSFD scheme (22) by mathematical induction.

Lemma 3. *The NSFD scheme* (22) *preserves the positivity of the model* (20) *for all values of the step size* Δt.

Using a similar approach, we can analyze the dynamical properties and construct NSFD schemes for the fractional versions of the model (2) under other fractional-order derivatives, e.g., the Riemann-Liouville fractional derivative operator [9, 18, 32, 52]. However, the analysis of the dynamical properties of the proposed NSFD schemes is in general not an easy task.

6. Discussions and conclusions

As the main conclusion of this work, we provided a generalized SEIR model to study the transmission dynamics of infectious diseases. The results obtained improved and extended those presented in the reference work [53] (see note 3). On the other hand, we constructed and analyzed a nonstandard numerical scheme capable of generating reliable approximations that preserve the dynamic properties of the SEIR model regardless of the step sizes chosen. Finally, a series of illustrative numerical experiments were also performed to support and illustrate the theoretical findings. The numerical results confirmed not only the validity of the theoretical findings, but also the advantages of the NSFD scheme over some well-known standard procedures.

Although the 2019 coronavirus disease pandemic (COVID-19) caused by severe acute respiratory syndrome coronavirus 2 (SARS-CoV-2) was controlled and prevented, mathematical modeling and analysis of the transmission dynamics of COVID-19 continues to play an essential role, not only in the post-CoVID-19 era but also in infectious disease research. This is an important basis for proposing effective disease control and public health planning strategies and interventions. Therefore, the proposed SEIR model will be useful in studying the COVID-19 epidemic in particular and other infectious diseases in general.

In the near future, we will investigate the generalized SEIR model (2) with vaccination to determine the effects of vaccines. Fractional order versions and parameter estimation problems with real life applications will also be studied. On the other hand, attention will be given to the construction of dynamically consistent high-order NSFD schemes for the SEIR model.

Ethical Approval: Not applicable.
Availability of supporting data: The data supporting the findings of this study are available within the article [and/or] its supplementary materials.
Conflicts of Interest: We have no conflicts of interest to disclose.
Funding information: Not available.
Authors' contributions:
M.T.H.: Conceptualization, Methodology, Software, Formal analysis, Writing-Original draft preparation
M.E.: Methodology, Analysis, Writing - Review & Editing, Supervision.

References

[1] N. Aguila-Camacho, A. M. Duarte-Mermoud, J. A. Gallegos, Lyapunov functions for fractional order systems, Communications in Nonlinear Science and Numerical Simulation 19 (2014) 2951-2957.

[2] N. Ahmed, A. Elsonbaty, A. Raza, M. Rafiq, W. Adel, Numerical simulation and stability analysis of a novel reaction-diffusion COVID-19 model, Nonlinear Dynamics 106 (2021) 1293-1310.

[3] L. J. S. Allen, An Introduction to mathematical biology, Pearson Education, Prentice Hall, 2007.

[4] L. J. S. Allen, P. van den Driessche, The basic reproduction number in some discrete-time epidemic models, Journal of Difference Equations and Applications 14 (2008) 1127-1147.

[5] R. Almeida, Analysis of a fractional SEIR model with treatment, Applied Mathematics Letters 84 (2018) 56-62.

[6] U. M. Ascher, L. R. Petzold, Computer Methods for Ordinary Differential Equations and Differential-Algebraic Equations, Society for Industrial and Applied Mathematics, Philadelphia, 1998.

[7] F. Brauer, P. Driessche, J. Wu, Mathematical Epidemiology, Springer-Verlag, Berlin Heidelberg, 2008.

[8] F. Brauer, Mathematical epidemiology: Past, present, and future, Infectious Disease Modelling 2 (2017) 113-127.

[9] M. Caputo, Linear models of dissipation whose Q is almost frequency independent-II, Geophysical Journal International 13 (1967) 529-539.

[10] L. C. Cardoso, R. F. Camargo, F. L. P. dos Santos, J. P. C. Dos Santos, Global stability analysis of a fractional differential system in hepatitis B, Chaos, Solitons & Fractals 143 (2021) 110619.

[11] G. Morais Rodrigues Costa, M. Lobosco, M. Ehrhardt, R.F. Reis, Mathematical Analysis and a Nonstandard Scheme for a Model of the Immune Response against COVID-19, in: A. Gumel (ed.), Mathematical and Computational Modeling of Phenomena Arising in Population Biology

and Nonlinear Oscillations: In honour of the 80th birthday of Ronald E. Mickens, AMS Contemporary Mathematics, 2023.

[12] J. Cresson, F. Pierret, Non standard finite difference scheme preserving dynamical properties, Journal of Computational and Applied Mathematics 303 (2016) 15-30.

[13] J. Cresson, A. Szafrańska, Discrete and continuous fractional persistence problems – the positivity property and applications, Communications in Nonlinear Science and Numerical Simulation 44 (2017) 424-448.

[14] Q. A. Dang, M. T. Hoang, Nonstandard finite difference schemes for a general predator-prey system, Journal of Computational Science 36 (2019) 101015.

[15] Q. A. Dang, M. T. Hoang, Positivity and global stability preserving NSFD schemes for a mixing propagation model of computer viruses, Journal of Computational and Applied Mathematics 374 (2020) 112753.

[16] Q. A. Dang, M. T. Hoang, Positive and elementary stable explicit nonstandard Runge-Kutta methods for a class of autonomous dynamical systems, International Journal of Computer Mathematics 97 (2020) 2036-2054.

[17] P. Das, R. K. Upadhyay, A. K. Misra, F. A. Rihan, P. Das, D. Ghosh, Mathematical model of COVID-19 with comorbidity and controlling using non-pharmaceutical interventions and vaccination, Nonlinear Dynamics 106 (2021) 1213-1227.

[18] K. Diethelm, The Analysis of Fractional Differential Equations: An Application-Oriented Exposition using Differential Operators of Caputo Type, Springer 2010.

[19] M. A. Duarte-Mermoud, N. Aguila-Camacho, A. J. Gallegos, R. Castro-Linares, Using general quadratic Lyapunov functions to prove Lyapunov uniform stability for fractional order systems, Communications in Nonlinear Science and Numerical Simulation 22 (2015) 650-659.

[20] M. Ehrhardt, J. Gašper, S. Kilianová, SIR-based Mathematical Modeling of Infectious Diseases with Vaccination and Waning Immunity, Journal of Computational Science 37 (2019) 101027.

[21] S. Elaydi, An Introduction to Difference Equations, Springer-Verlag, New York, 2005.

[22] H. Fatoorehchi, M. Ehrhardt, Numerical and semi-numerical solutions of a modified Thévenin model for calculating terminal voltage of battery cells, Journal of Energy Storage 45 (2022) 103746.

[23] C. Gan, X. Yang, W. Liu, Q. Zhu, X. Zhang, An epidemic model of computer viruses with vaccination and generalized nonlinear incidence rate, Applied Mathematics and Computation 222 (2013) 265-274.

[24] E. Hincal, S. H. Alsaadi, Stability analysis of fractional order model on corona transmission dynamics, Chaos, Solitons & Fractals 143 (2021) 110628.

[25] M. T. Hoang, A novel second-order nonstandard finite difference method for solving one-dimensional autonomous dynamical systems, Communications in Nonlinear Science and Numerical Simulation 114 (2022) 106654.

[26] M. T. Hoang, Positivity and boundedness preserving nonstandard finite difference schemes for solving Volterra's population growth model, Mathematics and Computers in Simulation 199 (2022) 359-373.

[27] M. T. Hoang, Reliable approximations for a hepatitis B virus model by nonstandard numerical schemes, Mathematics and Computers in Simulation 193 (2022) 32-56.

[28] M. T. Hoang, Dynamical analysis of a generalized hepatitis B epidemic model and its dynamically consistent discrete model, Mathematics and Computers in Simulation 205(2023) 291-314.

[29] M. T. Hoang, A class of second-order and dynamically consistent nonstandard finite difference schemes for nonlinear Volterra's population growth model, Computational and Applied Mathematics 42 (2023) Article number: 85.

[30] M. T. Hoang, M. Ehrhardt, A second-order nonstandard finite difference method for a general Rosenzweig-MacArthur predator-prey model, Preprint 23/07, University of Wuppertal, June 2023.

[31] O. Khyar, K. Allali, Global dynamics of a multi-strain SEIR epidemic model with general incidence rates: application to COVID-19 pandemic, Nonlinear Dynamics 102 (2020) 489-509.

[32] A. A. Kibas, H. M. Srivastava, J. J. Trujillo, Theory and Applications of Fractional Differential Equations, Elsevier Science, Inc., Volume 204, 1st Edition, 2006.

[33] W. Lacarbonara, J. Ma, C. Nataraj, Preface to the special issue "Complex dynamics of COVID-19: modeling, prediction and control (part II)", Nonlinear Dynamics 109(2022) 1-3.

[34] A. Lahrouz, L. Omari, D. Kiouach, A. Belmaâti, Complete global stability for an SIRS epidemic model with generalized non-linear incidence and vaccination, Applied Mathematics and Computation 218 (2012) 6519-6525.

[35] J. P. LaSalle, S. Lefschetz, Stability by Liapunov's Direct Method, Academic Press, New York, (1961).

[36] J. P. LaSalle, The Stability and Control of Discrete Processes, Applied Mathematical Sciences, Vol. 82, Springer-Verlag, New York, 1986.

[37] J. Li, Y. Yang, Y. Xiao, S. Liu, A class of Lyapunov functions and the global stability of some epidemic models with nonlinear incidence, Journal of Applied Analysis and Computation 6 (2016) 38-46.

[38] M. Y. Li, J. S. Muldowney, P. van den Driessche, Global stability of SEIRS models in epidemiology, Canadian Applied Mathematics Quarterly 7(4)(1999)

[39] M. Y.Li, J. S. Muldowney, Global stability for the SEIR model in epidemiology, Mathematical Biosciences 125 (1995) 155-164.

[40] Y. Li, Y. Chen, I. Podlubny, Mittag-Leffler stability of fractional order nonlinear dynamic systems, Automatica 45 (2009) 1965-1969.

[41] Y. Li, Y. Chen, I. Podlubny, Stability of fractional-order nonlinear dynamic systems: Lyapunov direct method and generalized Mittag-Leffler stability, Computers & Mathematics with Applications 59 (2010) 1810-1821.

[42] M. Martcheva, An Introduction to Mathematical Epidemiology, Springer New York, 2015.

[43] R. E. Mickens, Nonstandard Finite Difference Models of Differential Equations, World Scientific, 1993.

[44] R. E. Mickens, Applications of Nonstandard Finite Difference Schemes, World Scientific, 2000.

[45] R. E. Mickens, Nonstandard Finite Difference Schemes: Methodology and Applications, World Scientific, 2020.

[46] R. E. Mickens, I. H. Herron, Approximate rational solutions to the Thomas-Fermi equation based on dynamic consistency, Applied Mathematics Letters 116 (2021) 106994.

[47] J. Mondal, S. Khajanchi, Mathematical modeling and optimal intervention strategies of the COVID-19 outbreak, Nonlinear Dynamics 109 (2022) 177–202.

[48] R. Padmanabhan, H. S. Abed, N. Meskin, T. Khattab, M. Shraim, M. A. Al-Hitmi, A review of mathematical model-based scenario analysis and interventions for COVID-19, Computer Methods and Programs in Biomedicine 209 (2021) 106301.

[49] K. C. Patidar, On the use of nonstandard finite difference methods, Journal of Difference Equations and Applications 11 (2005) 735-758.

[50] K. C. Patidar, Nonstandard finite difference methods: recent trends and further developments, Journal of Difference Equations and Applications 22 (2016) 817-849.

[51] V. Piccirillo, Nonlinear control of infection spread based on a deterministic SEIR model, Chaos, Solitons & Fractals 149 (2021) 111051.

[52] I. Podlubny, Fractional Differential Equations, Academic Press, San Diego, 1999.

[53] G. Rohith, K. B. Devik, Dynamics and control of COVID-19 pandemic with nonlinear incidence rates, Nonlinear Dynamics 101 (2020) 2013-2026.

[54] H. L. Smith, P. Waltman, The Theory of the Chemostat: Dynamics of Microbial Competition, Cambridge University Press, 1995.

[55] P. van den Driessche, J. Watmough, Reproduction numbers and subthreshold endemic equilibria for compartmental models of disease transmission, Mathematical Biosciences 180 (2002) 29-48.

[56] C. Vargas-De-Leon, Volterra-type Lyapunov functions for fractional-order epidemic systems, Communications in Nonlinear Science and Numerical Simulation 24 (2015) 75-85.

[57] F. Wang, Y. Yang, Fractional order Barbalat's lemma and its applications in the stability of fractional order nonlinear systems, Mathematical Modelling and Analysis 22 (2017) 503-513.

[58] Q. Yang, X. Zhang, D. Jiang, Asymptotic behavior of a stochastic SIR model with general incidence rate and nonlinear Lévy jumps, Nonlinear Dynamics 107 (2022) 2975-2993.

[59] L. Zheng, X. Yang, L. Zhang, On global stability analysis for SEIRS models in epidemiology with nonlinear incidence rate function, International Journal of Biomathematics 20 (2017) 1750019.